

Provided for non-commercial research and education use.
Not for reproduction, distribution or commercial use.



This article appeared in a journal published by Elsevier. The attached copy is furnished to the author for internal non-commercial research and education use, including for instruction at the authors institution and sharing with colleagues.

Other uses, including reproduction and distribution, or selling or licensing copies, or posting to personal, institutional or third party websites are prohibited.

In most cases authors are permitted to post their version of the article (e.g. in Word or Tex form) to their personal website or institutional repository. Authors requiring further information regarding Elsevier's archiving and manuscript policies are encouraged to visit:

<http://www.elsevier.com/copyright>



Contents lists available at ScienceDirect

Journal of Non-Crystalline Solids

journal homepage: www.elsevier.com/locate/jnoncrsol

Letter to the Editor

Dissoluble and degradable CaLi-based metallic glasses

J.L. Li, D.Q. Zhao, M.X. Pan, W.H. Wang*

Institute of Physics, Chinese Academy of Sciences, Beijing 100190, China

ARTICLE INFO

Article history:

Received 17 October 2009

Received in revised form 16 August 2010

Available online 27 October 2010

Keywords:

Metallic glass;

Degradation

ABSTRACT

We study the degradable and dissoluble features of a Ca-Li-Mg-Zn bulk metallic glass in pure water at room temperature. A remarkable degradable feature of the metallic glasses is that the degradation is controllable by changing the composition and components. The degradable metallic glasses with superior combined properties of polymer-like thermal plasticity at low temperature (40–70 °C), the ultralow elastic moduli comparable to that of human bones, and ultralow density ($<2 \text{ g/cm}^3$) in known metallic glasses to date, and good machinability at a lower temperature in the supercooled liquid region could have potential applications. The metallic glasses also provide a model system to study the corrosion behavior in glasses.

© 2010 Elsevier B.V. All rights reserved.

As a neoteric material, metallic glasses, especially bulk metallic glasses (BMGs), are attractable since they exhibit appealing properties such as high strength and hardness, and high specific strength attribute to the absence of faults [1,2]. Their corrosion properties are also much more superior to their crystalline counterparts [3]. As a result, BMGs has been regarded as possible ideal structural materials, which have been applied in sporting equipment, magnetic materials and martial materials [4–7]. Furthermore, metallic glasses can be applied as coat to improve the corrosion resistance of materials [8]. On the other hand, the materials with degradable property are needed in biomaterial field contrasted to good corrosion resistance of metallic glasses [9]. However, the strength of these degradable materials is only as low as about 100 MPa [9–11]. Therefore, It is interesting if some metallic glasses with good mechanical properties combining dissoluble and degradable feature can be obtained. The BMGs combined excellent mechanical properties and degradable properties might be of importance both for basic research in glass sciences and potential applications.

Ca is classified to the VII groups of periodic table and has some unique properties such as low elastic moduli, low density, dissoluble and degradable, and biocompatible. So the Ca-based BMGs should have some unique properties according to elastic moduli criterion [5]. For example, it could be biomedical material for the constituted elements are biocompatible. The Ca-based BMGs are a rather new class of metallic glasses which were first reported in 2002 [12]. By introducing the Li element with the lowest elastic moduli (4.9 GPa) and density (0.525 g/cm^3) among all the metal elements into the Ca-based alloy, a serial of Ca-Li-Mg-Zn quaternary BMGs were developed. These alloys exhibit multiple properties, such as exceptionally low glass transition temperature

T_g ($\sim 35\text{--}60 \text{ }^\circ\text{C}$) approaching room temperature, the ultralow elastic moduli ($\sim 23 \text{ GPa}$) comparable to that of human bones, high elasticity (2%) and strength ($\sim 530 \text{ GPa}$), ultralow density ($<2 \text{ g/cm}^3$), exceptional thermodynamic and kinetic stability, strong liquid fragility similar to that of oxide glasses, ultrahigh specific strength ($\sim 270 \text{ MPa cm}^3 \text{ g}^{-1}$) and lower electrical resistivity ($\sim 44 \mu\Omega \text{ cm}$) at room temperature, and superplasticity and polymer-like thermoplastic formability in supercooled liquid region near room temperature [13].

In this letter, we study the degradation ability, the reaction rate and the surface image changes with time of CaLi-based BMGs immersed in the deionized water. Contrasts to other BMGs with high corrosion resistance, the CaLi-based BMGs have unique degradable and dissoluble properties even in pure water.

The Ca-Li-Mg-Zn quaternary alloys were prepared by induction melting of mixtures of Ca ($\geq 99 \text{ at.}\%$), pure Mg-Li alloy (containing 75 wt.%Mg) and pure Zn (99.9 at.%) in a quartz crucible in an argon atmosphere, and then cast into a copper mold to produce plate shapes samples. The structure of the as-cast and processed samples was examined by x-ray diffraction (XRD) using a MAC M03 XHF diffractometer with Cu- K_α radiation at 50 kV. The change of the surface morphologies of the sample was characterized by scanning-electron microscopy (SEM) and energy-dispersive spectroscopy (EDS) at an accelerated voltage of 10 keV. The degradable property was studied using static aqueous submersion at room temperature [14]. The sample was fixed using a human fair with a mass of 0.578 mg to measure its mass loss during the degradation process in deionized water. The degradable rate is evaluated by:

$$W = \frac{\Delta m}{S_0}, \Delta m = m_0 - \frac{m_w^t - m_f}{\rho_s - \rho_w} \cdot \rho_s \quad (1)$$

Δm , S_0 , m_w^t , m_f , ρ_s and ρ_w are mass change, the initial surface area of sample, the whole mass of sample and fair in the water at t time, the

* Corresponding author.

E-mail address: whw@aphy.iphy.ac.cn (W.H. Wang).

mass of fair, the density of sample and the density of water, respectively.

Fig. 1(a) shows that the CaLi-based BMGs have metallic shiny surfaces like other BMGs. The samples for water corrosion experiment were cut from an as-cast $\text{Ca}_{65}\text{Li}_{9.96}\text{Mg}_{8.54}\text{Zn}_{16.5}$ BMG plate, and its T_g is 317 K, and crystallization temperature T_x is 339 K. The density of the sample is 1.956 g/cm^3 , and the Young's modulus E , shear modulus G , bulk modulus K and Poisson's ratio of the BMG are 23.4 GPa, 8.95 GPa, 20.2 GPa and 0.307, respectively. The sample with an ultimate dimension of $1.38 \times 2.58 \times 10.44 \text{ mm}^3$ for degradable experiment was polished on 1000 grit emery paper without water rinse. The solution volume was 13.5 ml, and the S_0/V ratio (S_0 : the initial surface area of the sample; V : solution volume), which controlled the leaching kinetics, was 0.067 cm^{-1} . The little S_0/V ratio confined by the condition of experiment decelerated the kinetics [15]. The degradable kinetics was showed in the manner of real-time pictures of the water corrosion's process. Fig. 1(b) exhibits huge of gas bubbles immediately come into being in the water when the alloy was immersed into deionized water, and its surface lost metallic luster and the sample become darken soon. With increasing of the immersing time (4 to 20 h), the reacting productions can be seen clearly in the bottom (gray-black production) and on the top of the water (hoar production). The sample becomes smaller and smaller with the

increase of the reaction time. About 460 h, the sample broke to small parts, and finally the sample completely resolves into the water as shown in Fig. 1.

The degradable kinetics of the BMGs is also quantitative characterized. Fig. 2(a) shows the time dependence of the weight loss of the BMGs. The weight of $\text{Ca}_{65}\text{Li}_{9.96}\text{Mg}_{8.54}\text{Zn}_{16.5}$ BMG decreases rapidly in early reacting stage and becomes slower subsequently. After $\sim 106 \text{ h}$, the weight change (W_c) per unit area reaches 72% of the original sample mass. The dependence of W_c on the reacting time, t , shown insert of Fig. 2(a) was fitted by a parabolic relation:

$$W_c = at^{0.5} + b \quad (2)$$

where the rate constant $a = -7.03 \text{ mg}/(\text{cm}^2\text{s}^{0.5})$ and $b = 1.42 \times 10^{-14} \text{ mg/cm}^2$. The much larger a compared with that of $\text{Ca}_{65}\text{Mg}_{15}\text{Zn}_{20}$ BMG¹⁵ indicate that $\text{Ca}_{65}\text{Li}_{9.96}\text{Mg}_{8.54}\text{Zn}_{16.5}$ BMG was much more prone to degradation in water for the addition of active element lithium. Fig. 2(b) shows the X-ray analysis of the corrosion powder product of $\text{Ca}_{65}\text{Li}_{9.96}\text{Mg}_{8.54}\text{Zn}_{16.5}$ BMG. Three primary phases were identified, which are Calcium Hydroxide ($\text{Ca}(\text{OH})_2$), Calcium Zinc Hydroxide Hydrate ($\text{Ca}[\text{Zn}(\text{OH})_3]_2 \cdot \text{H}_2\text{O}$) and Zinc (Zn). Importantly,

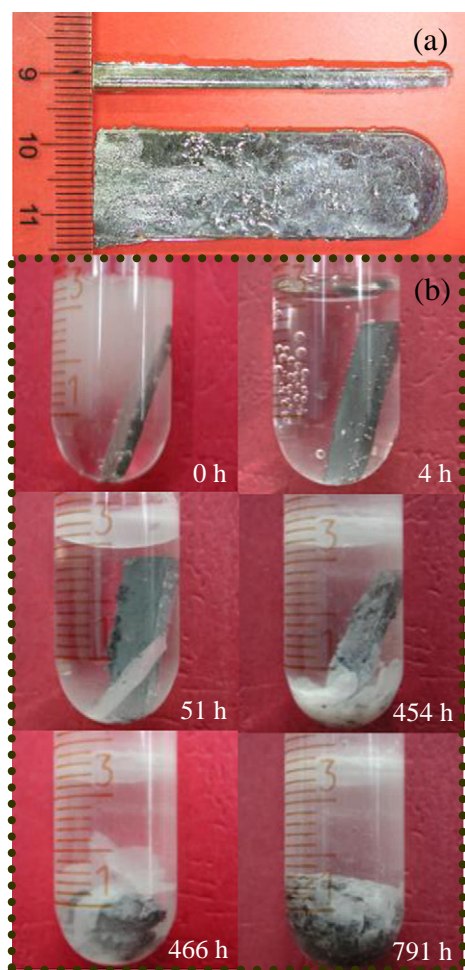


Fig. 1. (a) An as-cast $\text{Ca}_{65}\text{Mg}_{8.54}\text{Li}_{9.96}\text{Zn}_{16.5}$ glassy rod 3 mm in diameter, and a $\text{Ca}_{65}\text{Mg}_{8.54}\text{Li}_{9.96}\text{Zn}_{16.5}$ glassy sheet $2 \times 15 \times 50 \text{ mm}^3$. (b) The real-time pictures of the water corrosion's process of $\text{Ca}_{65}\text{Mg}_{8.54}\text{Li}_{9.96}\text{Zn}_{16.5}$ BMG.

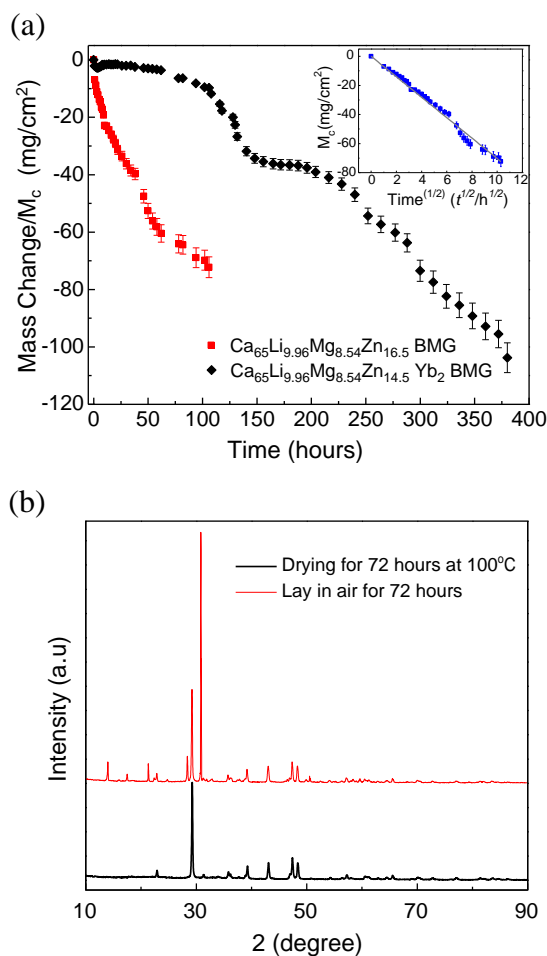


Fig. 2. (a) Weight changes per unit surface area of a $\text{Ca}_{65}\text{Li}_{9.96}\text{Mg}_{8.54}\text{Zn}_{16.5}$ and $\text{Ca}_{65}\text{Li}_{9.96}\text{Mg}_{8.54}\text{Zn}_{14.5}\text{Yb}_2$ BMGs versus holding time in deionized water. The inset shows the weight change per unit surface area of a $\text{Ca}_{65}\text{Li}_{9.96}\text{Mg}_{8.54}\text{Zn}_{16.5}$ (W_c) versus square root of holding time in deionized water (b) XRD of the reaction byproduct of $\text{Ca}_{65}\text{Li}_{9.96}\text{Mg}_{8.54}\text{Zn}_{16.5}$ BMG.

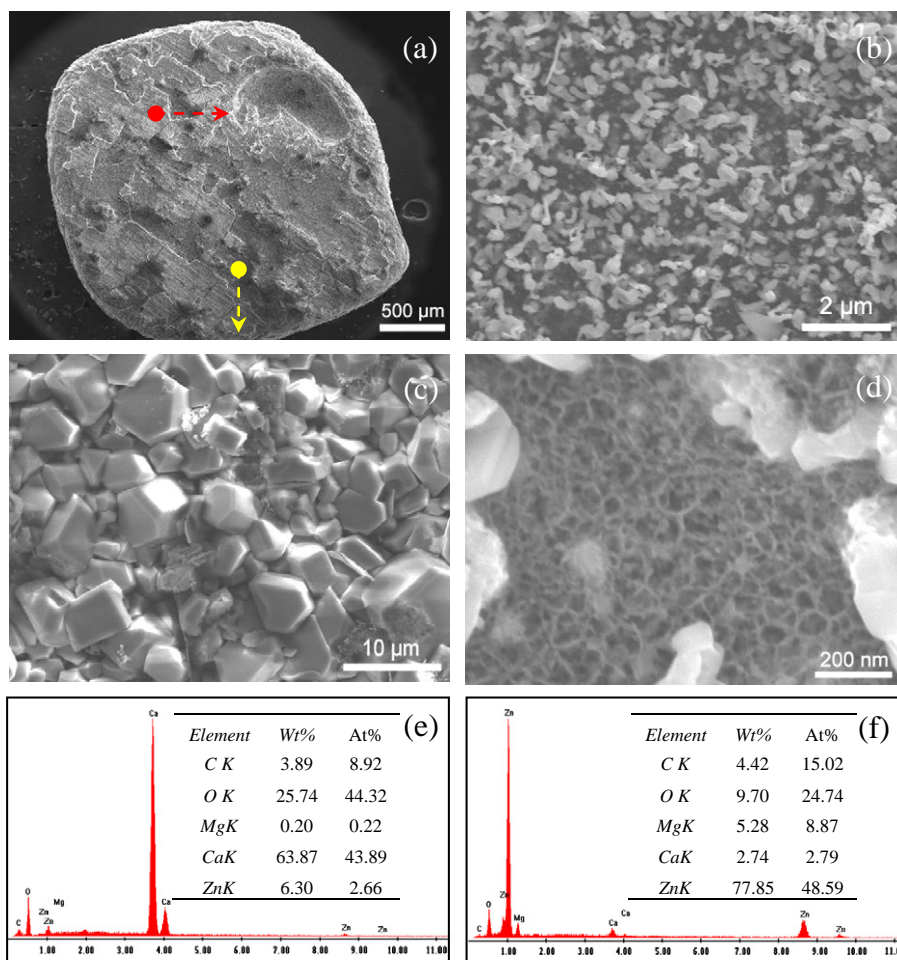


Fig. 3. (a) SEM image of morphology of $\text{Ca}_{65}\text{Li}_{9.96}\text{Mg}_{8.54}\text{Zn}_{16.5}$ BMG after immersing in deionized water for 4 h. (b) The surface morphology of the hatpacing zone of the $\text{Ca}_{65}\text{Li}_{9.96}\text{Mg}_{8.54}\text{Zn}_{16.5}$ BMG. (c) The surface morphology of the bottomland zone of the $\text{Ca}_{65}\text{Li}_{9.96}\text{Mg}_{8.54}\text{Zn}_{16.5}$ BMG. (d) The morphology of a local part of the hatpacing zone. (e) EDAX spectrum of the hatpacing zone. (f) EDAX spectrum of the bottomland zone.

the degradable ability can be modulated by change the composition of the BMGs. By minor addition of Ytterbium (Yb), the $\text{Ca}_{65}\text{Li}_{9.96}\text{Mg}_{8.54}\text{Zn}_{14.5}\text{Yb}_2$ BMG shows a much slower degradable process in the similar experiment condition as contrasted in Fig. 2(a). This indicates that minor addition can significantly improve the degradation behavior of the BMGs¹⁵.

SEM analysis of $\text{Ca}_{65}\text{Li}_{9.96}\text{Mg}_{8.54}\text{Zn}_{16.5}$ BMG alloy shows that surface morphology changing with the reacting time. The samples for SEM analysis had been polished before they were immersed into deionized water and rinsed in acetone by ultrasonic to wipe off the corrosion byproduct adhered to the samples surface. Fig. 3 shows the surface morphology after immersing in water for 4 h. The reaction with water is not homogeneous in the sample surface for its surface was unshaped with some hatpacing and bottomlands [Fig. 3(a)], and the micro-morphology is different at different places. The hatpacing zones are in nano-scale configuration ranging from hundreds nanometer [Fig. 3(b)] to dozens nanometer [Fig. 3(d)] and the bottomlands are micrometer-level structure [Fig. 3(c)]. EDAX shows the two zones have different chemical compositions. The hatpacing zones have a higher content of Ca and a lower content of Zn [Fig. 3(e)]. Correspondingly, the bottomland zones have a lower content of Ca and a higher content of Zn [Fig. 3(f)]. These indicated that there are different reacting rate at the different place of the sample.

The sample surface morphology after reacting with water for 8 h is antithetical to that of the sample after 4 h immersing. The hatpacing zones are micrometer-scale configuration [Fig. 4(b)] and the bottomlands are micro-nano meter scale structure [Fig. 4(c)–(d)]. And the bottomlands show a stalactitic surface morphology. EDAX showed the two zones exhibit slight different in chemical composition. The hatpacing zones have a higher atom ratio of Ca/Zn than the bottomland zones which has a higher content of Zn element [in Fig. 4(e)–(f)]. The different surface morphology of the sample after reacting with water indicates one can modify the surface of the BMG to control the corrosion resistivity and hydrophobicity and so on [16,17].

Contrasting to the traditional biomaterials [18], CaLi-based BMGs have properties combined with low elastic moduli, low density, and biocompatible. Furthermore, CaLi-based BMGs have the higher strength as an alloy, good machinability at a lower temperature in the supercooled liquid region (for details see Ref. [13]). The good and modulated degradable ability distinct to traditional metallic glasses make the BMG a potential biomaterial [19,20]. The BMGs also provide a model system for studying the corrosion mechanism of the metallic glasses.

Thanks X. X. Xia for the help of SEM experiment. The financial support from the NSFC of China (Nos. 50621061 and 50731008) and MOST 973 of China (Grant Nr. 2007CB613904) are acknowledged.

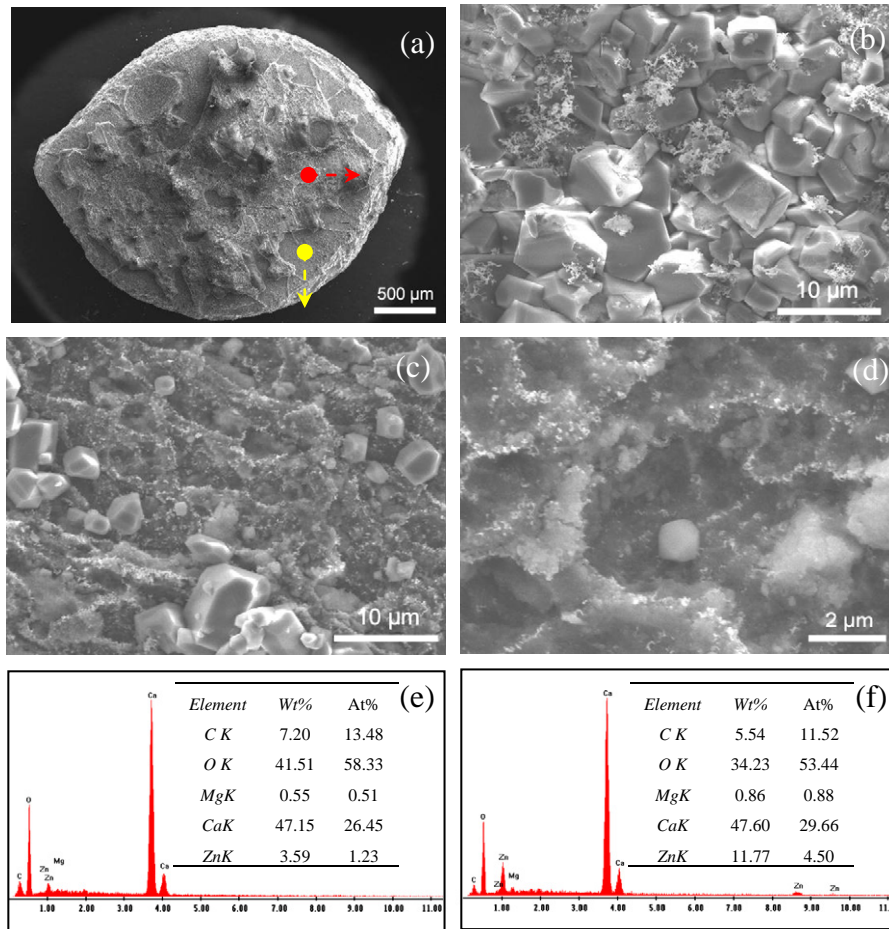


Fig. 4. (a) SEM image of the morphology of the $\text{Ca}_{65}\text{Li}_{9.96}\text{Mg}_{8.54}\text{Zn}_{16.5}$ BMG sample after immersing in deionized water for 8 h. (b) The surface morphology of the hathpace zone of the $\text{Ca}_{65}\text{Li}_{9.96}\text{Mg}_{8.54}\text{Zn}_{16.5}$ BMG. (c) The surface morphology of the bottomland zone. (d) The morphology of a local part of the bottomland zone. (e) EDAX spectrum of the hathpace zone. (f) EDAX spectrum of the bottomland zone.

References

- [1] F. Spaepen, *Science* 235 (1987) 1010.
- [2] A.L. Greer, *Science* 267 (1995) 1947.
- [3] J.J. Gilman, *Science* 208 (1980) 856.
- [4] (a) W.H. Wang, *Prog. Mater. Sci.* 52 (2007) 540;
(b) W.H. Wang, *Adv. Mater.* 21 (2009) 4524;
(c) Q. Luo, W.H. Wang, *J Non-cryst Solids* 355 (2009) 759.
- [5] (a) W.H. Wang, *J. Appl. Phys.* 99 (2006) 093506;
(b) B. Zhang, D.Q. Zhao, M.X. Pan, W.H. Wang, A. Lindsay Greer, *Phys. Rev. Lett.* 94 (2005) 205502.
- [6] W.L. Johnson, *MRS Bull.* 24 (1999) 42.
- [7] A. Inoue, *Bulk Amorphous Alloys*, Trans Tech Publications, Zurich, 1998–1999.
- [8] Y.H. Yoo, S.H. Lee, J.G. Kim, J.S. Kim, C. Lee, *J. Alloys Compd.* 461 (2008) 304.
- [9] Z.J. Li, X.N. Gu, S.Q. Lou, Y.F. Zheng, *Biomaterials* 29 (2008) 1329.
- [10] M.M. Avedesian, H. Baker, *Magnesium and magnesium alloys*, ASM specialty handbook, The Mater. Infor. Soc, ASM International, 1999.
- [11] Y. Shikinamia, M. Okuno, *Biomaterials* 20 (1999) 859.
- [12] K. Amiya, A. Inoue, *Mater. Trans., JIM* 43 (2002) 81.
- [13] (a) J.F. Li, D.Q. Zhao, M.L. Zhang, W.H. Wang, *Appl. Phys. Lett.* 93 (2008) 171907;
(b) K. Zhao, K.S. Liu, J.F. Li, W.H. Wang, L. Jiang, *Scr. Mater.* 60 (2009) 225.
- [14] K. Zhao, J.F. Li, D.Q. Zhao, M.X. Pan, W.H. Wang, *Scr. Mater.* 61 (2009) 1091.
- [15] J. Dahlman, O.N. Senkov, J.M. Scott, D.B. Miracle, *Mater. Trans., JIM* 48 (2007) 1850.
- [16] P.K. Chu, J.Y. Chen, L.P. Wang, N. Huang, *Mater. Sci. Eng. R.* 36 (2002) 143.
- [17] K.S. Liu, M.L. Zhang, J. Zhai, J. Wang, L. Jiang, *Appl. Phys. Lett.* 92 (2008) 183103.
- [18] J. Black, G. Hastings, *Handbook of Biomaterial Properties*, Chapman & Hall, London, 1998.
- [19] B. Zberg, P.J. Uggowitzer, J.F. Löffler, *Nature Mater.* 8 (2009) 887.
- [20] L.G. Griffith, *Acta Mater.* 48 (2000) 263.